Adsorption 6, 275–286, 2000

Comparison of Experimental Techniques for Measuring Isosteric Heat of Adsorption

DONGMIN SHEN AND MARTIN BÜLOW
The BOC Group, Murray Hill, NJ 07974, USA

FLOR SIPERSTEIN, MAXIMILIAN ENGELHARD AND ALAN L. MYERS
University of Pennsylvania, Department of Chemical Engineering,
University of Pennsylvania, PA 19104, USA

Abstract. Experimental measurements of heats of adsorption published in the literature are often in disagreement; differences of 10–20% are common. The three most widely used experimental methods are: (1) differentiation of adsorption isotherms at constant loading; (2) measurement of adsorption isosteres; (3) calorimetry. Results from these methods were compared for the systems nitrogen on CaA, oxygen on CaA, and carbon dioxide on NaX. Although the same materials and similar degassing procedures were used for all experiments, calorimetric heats are about 2 kJ/mol higher than the heats from isoteric measurements. Additional experiments are needed to bring these methods into exact agreement.

Keywords: sorption heats, calorimetry, isosteric technique, zeolites, gases

1. Introduction

Zeolites of the CaA-type were the first generation of sorbents in pressure-swing-adsorption (PSA) systems for oxygen production in the early 1970s. Since then, further development has led to major improvements in both sorbents and processes. In the early 1980s, the second generation of oxygen PSA sorbents with higher selectivity and capacity, e.g., NaX and CaX zeolites, were introduced into industrial plants. Their utilization resulted in modern VSA processes with a significant reduction of capital costs. In the 1990s, utilization of lithium-containing molecular sieves, e.g., LiX, Li,Me^{2+}X and Li,Me^{3+}X (McKee, 1964; Coe et al., 1993; Fitch et al., 1995), where Me is a metal atom, has enabled a power cost reduction and a significant increase in oxygen yield.

Despite wide industrial utilization of oxygen PSA and vacuum swing adsorption (VSA) processes, little information is available in the literature on sorption of N_2-O_2 mixtures in microporous sorbents. Those data which have been reported, especially isosteric heats, are frequently contradictory (Valenzuela and Myers, 1989). A reference system which yields the same results when measured by different methods and by different investigators is needed for calibration of instruments. In this paper, sorption thermodynamics for N_2 and O_2 on CaA, and CO_2 on NaX are based on experimental results obtained using the isosteric (Bülow and Lorenz 1987; Bülow, 1994; Shen and Bülow, 1998) and calorimetric (Dunne et al., 1996a; Dunne et al., 1996b; Siperstein et al., 1996) techniques. Comparing sorption heats obtained by these two methods is a first step toward the establishment of a reference system.

2. Isosteric Heat

The objective of this work is to compare isosteric heats of adsorption measured by different techniques. The thermodynamic definition of the isosteric heat of a pure gas is the molar enthalpy in the gas phase minus the differential enthalpy in the adsorbed phase:

$$q_{\mathrm{st}} = h^{\mathrm{g}} - \left[\frac{\partial H^{\mathrm{m}}}{\partial n^{\mathrm{m}}}\right]_T \tag{1}$$

where H^{m} is the specific enthalpy [J/kg] of the adsorbed phase and n^{m} is the specific amount adsorbed [mol/kg]. The $^{\mathrm{m}}$ superscript denotes that the variables are *measured* Gibbs excess variables (Sircar, 1985); absolute values calculated by molecular simulation must be converted to excess variables for comparison with experiment. For a real gas, the isothermal variation of its enthalpy with pressure introduces residual enthalpy nuisance terms into the thermodynamic equations. Since our experiments are performed at subatmospheric pressure, the following equations are written for the case when the bulk gas obeys the perfect gas law. It can then be shown that Eq. (1) is equivalent to:

$$q_{\mathrm{st}} = -R\left[\frac{\partial \ln P}{\partial(1/T)}\right]_{n^{\mathrm{m}}} \tag{2}$$

Plots of $\ln P$ as a function of reciprocal absolute temperature at constant loading are called adsorption isosteres; Eq. (2) shows that the isosteric heat is determined by their slope.

A second method of measuring the isosteric heat is calorimetry. The working equations depend upon the design of the apparatus, but for an isothermal calorimeter:

$$-q_{\mathrm{st}} = \frac{Q + V^t \Delta P}{\Delta n^{\mathrm{m}}} \tag{3}$$

where Q is the heat registered [J/kg] for an incremental dose of gas Δn^{m} introduced at the temperature of the calorimeter cell. Since adsorption is exothermic, Q is negative. V^t [m^3/kg] is the dead space in the sample cell; the $V^t \Delta P$ term in Eq. (3) is small compared to Q.

3. Heat Capacity

Sorption heats calculated from adsorption isosteres by Eq. (2) are average values for the range of temperature covered by the isostere. In this section, the variation of the heat of sorption with temperature is considered in terms of heat capacities. It is generally accepted that sorption heats are constant over some range of temperature, but little is known about the accuracy of the approximation. Whether the isosteric heat increases or decreases with temperature is also unknown.

We define a difference of heat capacities at constant loading (ΔC_n) by:

$$\Delta C_n = \left(\frac{\partial q_{\mathrm{st}}}{\partial T}\right)_n \tag{4}$$

Substitution of Eq. (1) in (4) shows that ΔC_n is the difference of two heat capacities: the gas-phase heat capacity (C_p) less the differential heat capacity in the adsorbed phase.

Since experimental data are unavailable, we calculated isosteric heats for idealized geometries by differentiating the adsorption second virial coefficient (B_{1S}) with respect to temperature. The smeared potential approximation was used for the surface atoms on a flat surface, in a cylindrical pore, and in a spherical pore (Everett and Powl, 1976). Since the model surfaces are energetically homogeneous, the results should apply to argon or methane on silicalite. Our calculations show that the isosteric heat increases with temperature and the dimensionless quantity $\Delta C_n/R$ is positive but less than unity for energetically homogeneous systems.

Systems such as carbon dioxide sorbed in NaX display energetic heterogeneity induced by high energy sites adjacent to the sodium cations and low energy sites elsewhere in the supercage. The heat of adsorption at low temperature decreases with loading as the high energy sites are filled first. At high temperature, the heat of adsorption is equal to the average value and is almost independent of loading in accordance with the Boltzmann exponential probability distribution. Therefore at low coverage the heat of adsorption decreases with temperature and at high coverage the heat of adsorption increases with temperature. The quantity ΔC_n is negative at low coverage and positive at high coverage and the (negative) value is largest at the limit of zero coverage. Experimentally, as reported below, our calorimetric measurements at the limit of zero coverage yield $\Delta C_n = -3R$ for oxygen adsorbed on CaA and $\Delta C_n = -5R$ for nitrogen adsorbed on CaA.

In summary, the variation of isosteric heat with temperature is of order $-5R$ for heterogeneous systems at the limit of zero coverage. The variation of isosteric heat with temperature is of order R for homogeneous systems at the limit of zero coverage.

4. Materials

Two adsorbents were used in this study: CaA and NaX. Both zeolites are formed from sodalite cages joined by four-membered (CaA) or six-membered (NaX) double rings. The supercages (α-cages) have windows formed by 8 (CaA) and 12 (NaX) T-atoms (Meier and Olson, 1992). The CaA zeolite sample was prepared by A.F. Ojo (BOC Gases Technology) by means of a fourfold Ca^{2+} ion exchange process on NaA zeolite powder

Table 1. Composition of CaA zeolite measured by ICP analysis.

Compound	Wt %
LOI	23.58
Al_2O_3	27.00
SiO_2	33.22
Na_2O	<0.1
K_2O	<0.1
CaO	15.05
Total	99.05

using aqueous $CaCl_2$ solution. The original NaA zeolite showed an excellent XRD powder pattern and therefore had a high degree of crystallinity. The chemical composition of the CaA zeolite determined by Inductive Coupled Plasma Spectroscopy is listed in Table 1. The NaX zeolite was commercial 13X from UOP Company with a Si/Al ratio of 1.2 and pelletized with 20% inert binder according to the commercial product specifications.

5. Measurement of Heat of Sorption by Isosteric Technique

The sorption isosteric technique (SIT) was applied to two zeolites: N_2 and O_2 on CaA zeolite, pelletized but binderless; and CO_2 on NaX pellets with 20% binder. A detailed description of this technique and its utilization for an investigation of sorption thermodynamic properties of noble gases and N_2, O_2, and CO_2 on various microporous materials has been reported previously (Bülow and Lorenz, 1987; Bülow, 1994; Shen and Bülow, 1998).

The SIT technique is based upon Eq. (2). The experimental procedure relies on the experience of isostere linearity that holds over very broad temperature and pressure regions the limits of which may even exceed critical pressures and temperatures if no sorption phase transition takes place. The method takes into account that any experimental mistake such as (i) a disturbance of the isosteric condition; or (ii) restricted pressure sensor resolution/sensitivity; leads to a lower slope of the curve $\ln P$ vs. $(1/T)$ and, thus, a deviation from linearity. In case (i), the curve $\ln P$ vs. $(1/T)$ usually deviates to an equilibrium pressure lower than suggested by linear prolongation of the isostere into the region of higher pressure values. In case (ii), deviations to a lower slope may occur at the low-pressure end of the experimental $\ln P$ vs. $(1/T)$ curve. Since such situations become obvious during data acquisition where much attention has to be paid to the equilibration of the sorption system, erroneous regions of plots of $\ln P$ vs. $(1/T)$ can be recognized easily. The sources of error are best illustrated by an example based upon experimental data.

Analysis of Method of Adsorption Isosteres

The isosteric method is based on the measurement of pressure and temperature in a closed system of known volume containing a known amount of gas (n^t) and a known mass of adsorbent but only a small dead space. For a perfect gas, the mass balance for the excess amount adsorbed n^{m} is:

$$n^t = n^{\mathrm{m}} + \frac{PV^t}{RT} \tag{5}$$

V^t is the dead space in the sample cell determined by low pressure, room temperature helium measurements. In the limit of zero dead space V^t in Eq. (5), all of the gas is adsorbed and therefore remains constant for the complete isostere. Of course, in an actual experiment the strategy is to minimize the dead space so that the amount of gas adsorbed (n^{m}) always remains a high percentage of the total amount in the cell (n^t) over the temperature range considered.

Figure 1 shows isosteres calculated for different dead space values using experimental data for a gas adsorbed weakly at room temperature (CH_4 on silicalite–1 (Dunne et al., 1996a)) and a gas adsorbed strongly at room temperature (CO_2 on NaX (Dunne et al., 1996b)). The points were calculated from experimental isotherms and heats of adsorption using the integrated form of Eq. (2) and assuming that q_{st} is independent of temperature over the range of the isostere. Figure 1(A) is for high coverage and Fig. 1(B) is for low coverage. In each case, the solid line is for the desirable but unattainable limit of zero dead space. The closed symbols are for a small dead space (1.8 cm^3/g) and the open symbols are for a large dead space (18 cm^3/g). It is evident that at low pressure (or low temperature) the isosteric method gives the correct slope for the isosteric heat, but as pressure increases the isostere eventually starts to bend. As stated previously, the correct heat is given by the maximum slope (the solid lines). The importance of minimizing the dead space is apparent.

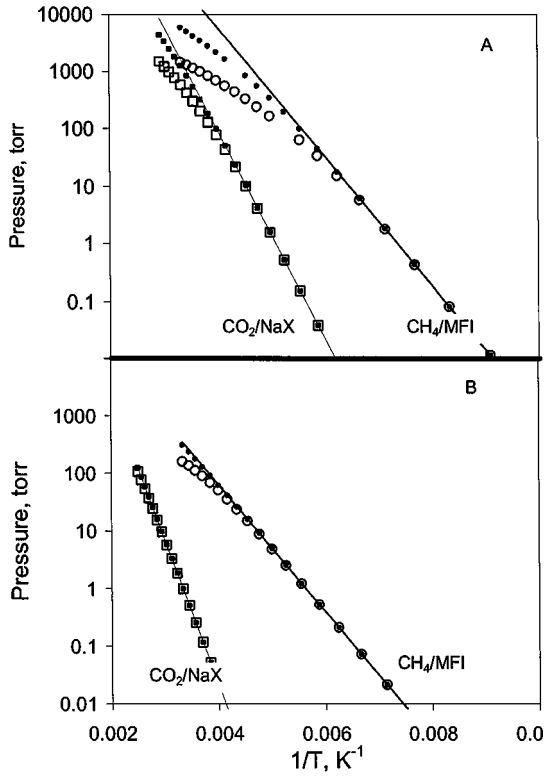

Figure 1. Calculated isosteres for CO_2 on NaX (squares) and CH_4 on silicalite–1 (circles) for dead space values of zero (solid line), 1.8 cm^3/g (solid symbols), and 18 cm^3/g (open symbols). (A) High loading: 6.1 mol/kg for CO_2 and 2.3 mol/kg for CH_4. (B) Low loading: 0.8 mol/kg for CO_2 and 0.3 mol/kg for CH_4.

Sircar (1992) derived equations to calculate the error in heats of sorption and showed that the method may give large errors in slopes of isosteres if utilized uncritically. It is important to bear in mind that the determination of heats of sorption by the method of isosteres is *not* based on measuring the slope at individual points. Instead, the measured slope is a best-fit straight line through all of the points. For example, for methane adsorbed on silicalite–1 and for a dead space of 1.8 cm^3/g, a pressure of 100 torr, and a loading of 2.3 mol/kg, the isosteric heat is 21.55 kJ/mol and the heat calculated from the slope of the isostere by Eq. (2) is 19.82 kJ/mol, an error of about 10%. However, a straight line drawn from a low pressure (0.1 torr) to 100 torr yields an isosteric heat of 21.28 kJ/mol, an error of about 1%.

The important factors which influence the error in the isosteric method are the dead space, the minimum attainable pressure, and the application of a reasonable

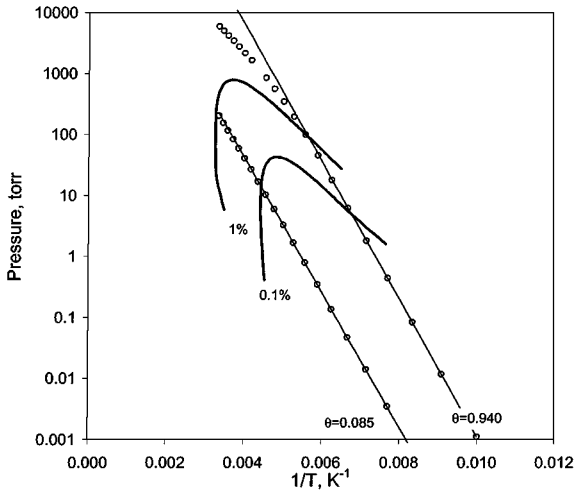

Figure 2. Calculated isosteres for CH_4 on silicalite–1 at loadings of 0.2 mol/kg and 2.3 mol/kg. The cutoff lines indicate the maximum pressure for errors of 0.1% and 1% based on a minimum pressure of 0.001 torr and a dead space of 1.8 cm^3/g.

cutoff for the maximum pressure (or maximum temperature) for a given loading. Figure 2 shows the maximum allowable pressure (and maximum temperature) for restricting the error to 0.1% and 1% for methane adsorbed on silicalite–1.

Sorption of N_2 and O_2 on CaA

The CaA zeolite crystals were pelletized and sieved into particles about 1.5 mm in diameter. The mass of the sample in the sorption vessel was 6.2997 g (dry weight) and the dead space was 3.809 cm^3/g. Isosteric measurements were performed over regions of temperature from 60–250 K and 70–200 K, respectively, for N_2 and O_2, at sorbate equilibrium pressures from 0.1–100 torr. Altogether, 18 and 19 isosteres were obtained for N_2 and O_2, respectively. The dosing was manipulated to cover sorption concentration ranges of N_2 and O_2 from 0.06–8.00 mol/kg and 0.05–8.05 mol/kg, respectively. For the isosteric experiments, an experimental determination of isosteric heats below 0.05 mol/kg could not be achieved because of instabilities in the measurement of pressure.

Sorption of CO_2 on NaX

A dry mass of 6.5484 g of NaX pellets with 20% binder was used. The dead space was 3.665 cm^3/g. Isosteres were measured for a range of temperatures between

155–310 K and pressures between 0.01 to 100 torr. Seventeen isosteres were measured for coverages ranging between 0.2–8.9 mol/kg. The accuracy of measurements expressed in terms of heat of sorption is ±100 J/mol for the three systems studied. For each of the three systems, at least 60 minutes were allowed for equilibration of each point of the isostere while monitoring changes in both temperature and pressure.

Results

Sorption isosteres measured for the systems N_2/CaA, O_2/CaA, and CO_2/NaX are presented in Figs. 3–5. In these plots of $\ln P$ vs. $(1/T)$, the isosteres for a low sorption phase concentration appear on the left-hand-side. The sorption phase concentration increases stepwise to the right for each isostere because for a given temperature, the equilibrium pressure in the gas phase increases with the sorption phase concentration. The slope of these isosteres changes with sorption phase concentration if the sorption heat depends on the latter. The linear sorption isosteres imply that no sorption phase transitions occurred. Isosteric heats were calculated from Eq. (2). Table 2 lists values of the total loadings with values of the corresponding isosteric heat.

6. Measurement of Heat of Sorption by Calorimetry

A Tian-Calvet calorimeter used to measure isotherms and heats of sorption simultaneously at room temperature has been described before (Dunne et al., 1996a; Dunne et al., 1996b; Siperstein et al., 1999). Some modifications were made to operate at low temperatures in order to measure higher loadings for N_2 and O_2. The

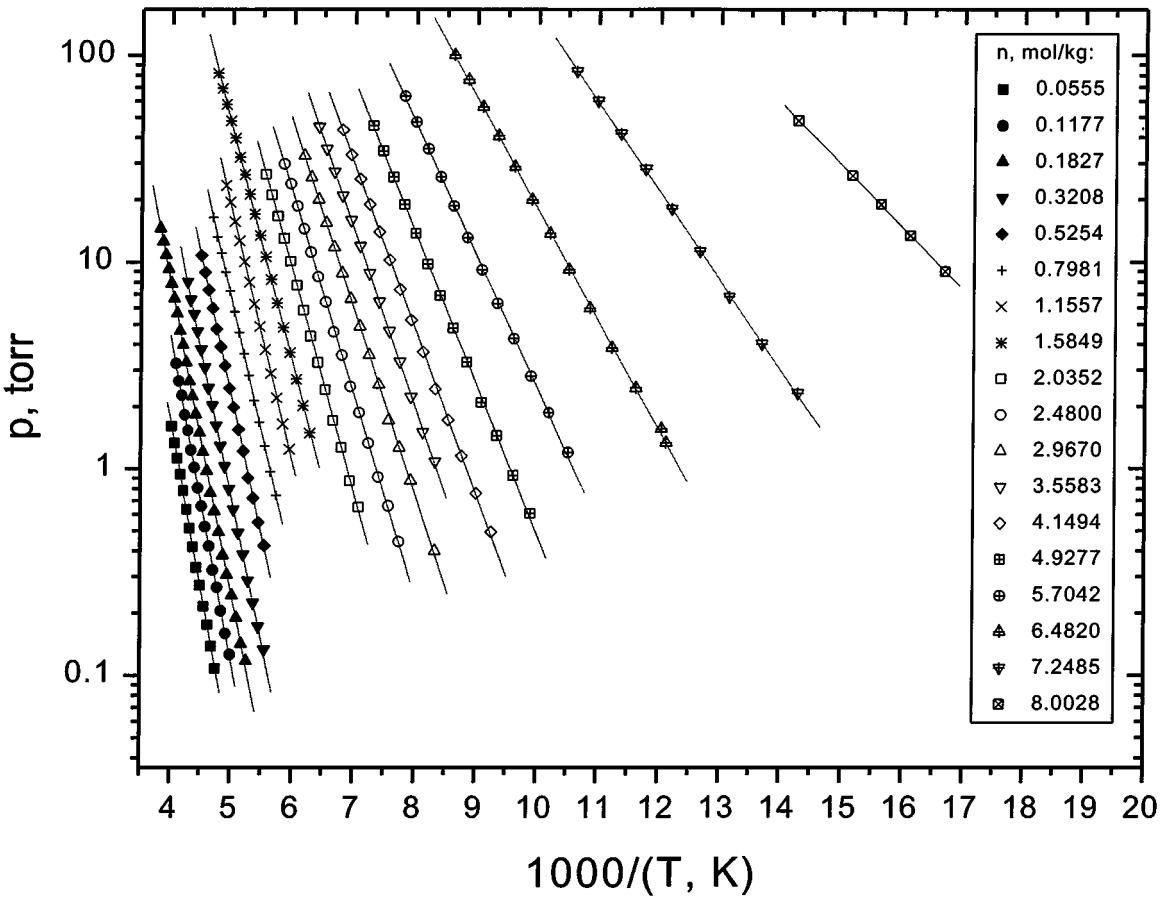

Figure 3. Sorption isosteres for nitrogen on CaA zeolite.

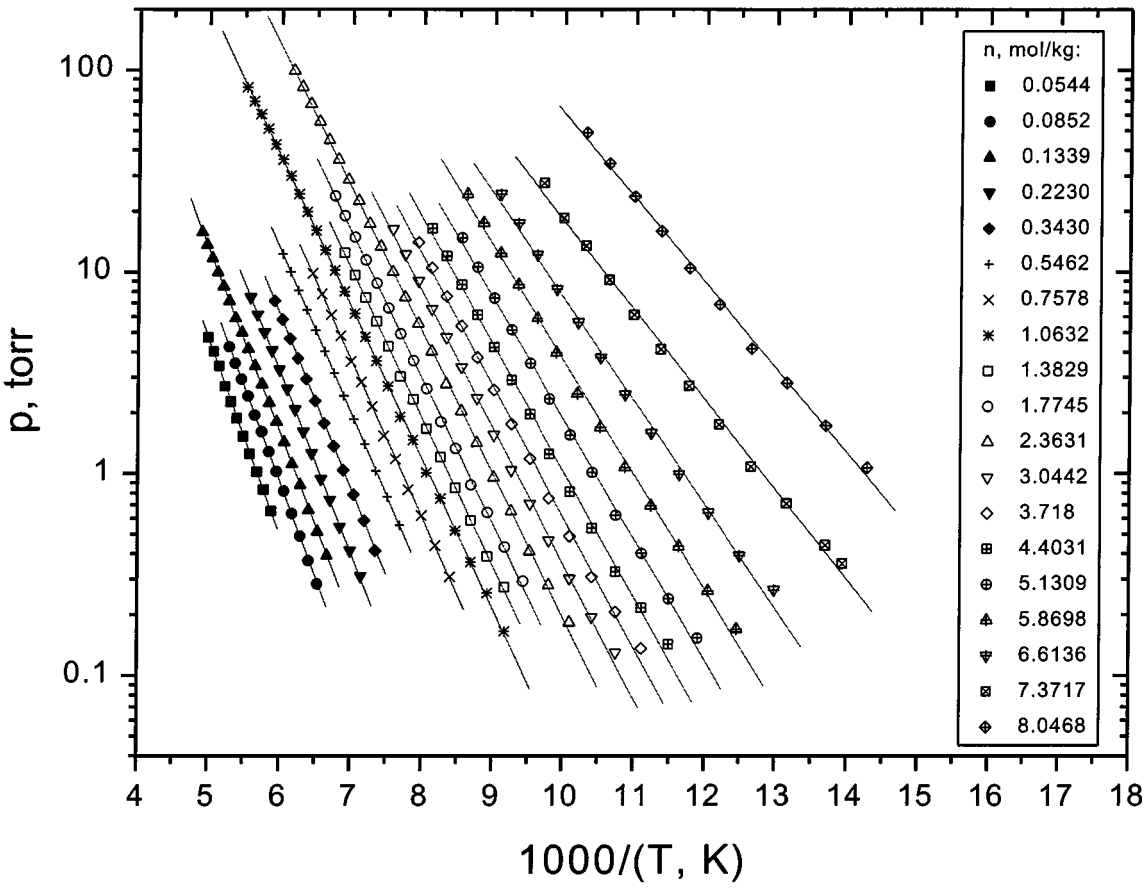

Figure 4. Sorption isosteres for oxygen on CaA zeolite.

heart of the calorimeter consists of a cubical Pyrex cell which serves as a sample chamber and is encased on 5 of its 6 sides by thermopiles. The cell, which sits in an aluminum block that acts as a heat sink, is connected to the dosing loop and vacuum through a custom made T-shaped fitting.

For low temperature operation, the isothermal enclosure was filled with solid CO_2 up to the top of the aluminum block. At least 12 hours are allowed for temperature equilibration after introducing the dry ice. Since isosteric heats of a non-polar gas on a homogeneous adsorbent are nearly independent of temperature as discussed previously, the calorimeter was calibrated with the system C_2H_6 on silicalite–1 by assuming that the isosteric heat was independent of temperature over the range 195 to 298 K. Based upon this assumption, the calibration constant of 0.06744 W/mV at 298 K was found to be 0.07609 W/mV at 195 K. We were unable to obtain information about the temperature dependence of the thermopile signal with temperature and thus check the calibration constant. The thermopile manufacturer (International Thermal Instruments Co.) claims that the signal is independent of temperature in a range from 0 to 250°C but information about the signal at low temperature is unavailable. The thermopiles are arrays of gold-constantan thermocouples but we were unable to find calibration curves for this thermocouple. For thermocouples T (copper/copper-nickel) and K (nickel-chromium/nickel-aluminum) calibration constants at 195 K should be 28% and 16% higher than at 295 K, respectively. Therefore our difference in calibration constants (13%) is reasonable.

The expansion of the gas into the cell is accompanied by a cooling of the dosing loop and heating of the cell. This effect was measured at 298 and 195 K on a blank cell using different gases. The heat due to the compression of the gas is proportional to the difference in pressures between the cell and the dosing loop. No

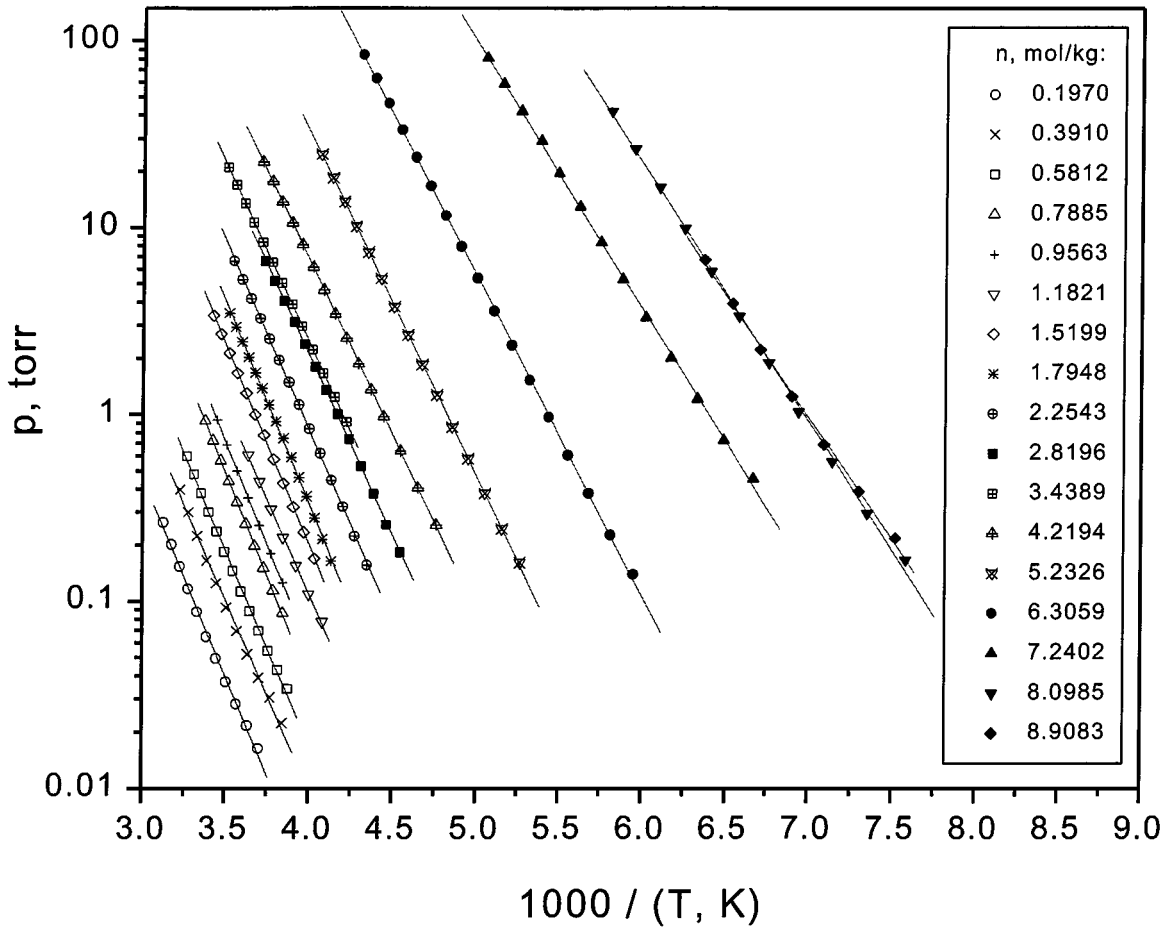

Figure 5. Sorption isosteres for carbon dioxide on NaX zeolite.

appreciable difference was observed for different gases or for different temperatures in the correction for this spurious compression effect.

Sorption of N_2 and O_2 on CaA

Zeolite powder was pressed into thin wafers; approximately 1 g of hydrated zeolite was placed in the calorimeter cell, heated under vacuum from room temperature to 110°C in 12 hours, then ramped to 350°C in 12 hours, and then held at 350°C for another 12 hours.

The dead space value in the cell was determined using helium expansions at room temperature. The sample was again evacuated for at least 6 hours and dry ice was added to cool the system to 195 K. Isosteric heats were measured for N_2 and O_2 by adding incremental amounts of gas to the sample cell up to loadings of 3.4 and 2.4 mol/kg, respectively. Time allowed for equilibration was at least 25 minutes for each point. The heat liberated by the sorption of an incremental Δn moles of gas was determined by integrating the area under the response curve generated by the thermopiles. Adsorption isotherms at 195 K generated during the calorimeter run are shown on Fig. 6, where they are compared with values interpolated from the adsorption isosteres plotted on Figs. 3 and 4. The agreement is excellent.

Sorption of CO_2 on NaX

Heats of adsorption for CO_2 on NaX pellets with 20% binder were measured at 25°C using a room temperature calorimeter (Dunne et al., 1996a; Dunne et al., 1996b; Siperstein et al., 1999). The degassing

Table 2. Isosteric heats of adsorption of N_2 and O_2 on CaA and CO_2 on NaX.

N_2 on CaA		O_2 on CaA		CO_2 on NaX	
n, mol/kg	q_{st}, kJ/mol	n, mol/kg	q_{st}, kJ/mol	n, mol/kg	q_{st}, kJ/mol
0.056	31.2	0.054	19.2	0.197	44.2
0.118	30.2	0.085	18.4	0.391	43.4
0.183	29.1	0.134	17.9	0.581	42.9
0.321	27.5	0.223	17.4	0.789	42.3
0.525	26.1	0.343	16.5	0.956	41.9
0.798	25.1	0.546	15.5	1.182	40.6
1.156	23.5	0.758	15.1	1.520	40.4
1.585	22.3	1.063	14.7	1.795	39.7
2.035	20.6	1.383	14.3	2.254	38.6
2.480	18.9	1.775	14.2	2.820	37.2
2.967	17.4	2.363	13.9	3.439	36.8
3.558	16.5	3.044	13.6	4.219	36.0
4.149	15.6	3.718	13.0	5.233	35.3
4.928	14.2	4.403	12.7	6.306	32.7
5.704	12.5	5.131	12.2	7.240	28.0
6.482	10.5	5.870	11.7	8.099	27.0
7.249	8.4	6.614	10.6	8.908	26.6
8.003	5.8	7.372	9.2		
		8.045	8.5		

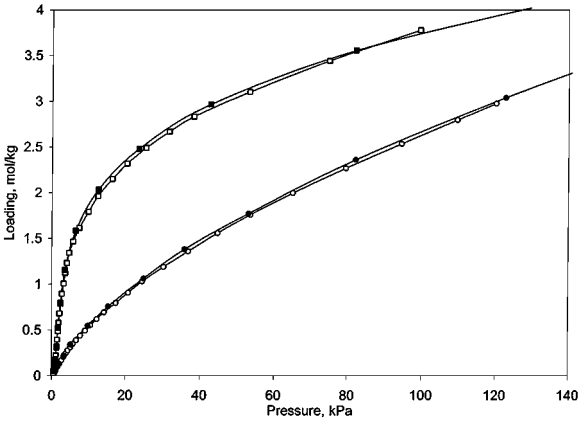

Figure 6. Comparison of isotherms at 195 K for N_2 (squares) and O_2 on CaA (circles) from calorimeter run (open points) and from SIT runs (closed points).

procedure was similar to the one used for CaA: the sample was heated under vacuum from room temperature to 110°C in 24 hours, ramped to 400°C in 12 hours, and then held at 400°C for another 12 hours.

Isosteric Heats

Isosteric heats of sorption for N_2 and O_2 on CaA measured with the calorimeter at 195 K, and for CO_2 on NaX with the room temperature calorimeter at 298 K, are listed in Table 3. Sorption heats for N_2 are higher than for O_2. This finding had been addressed in detail, recently (Shen et al., 1999). For N_2, the heats decrease continuously with coverage but the O_2 heats decrease at low coverage and reach a plateau at loadings above

Table 3. Calorimetric heats of adsorption of N_2 and O_2 on CaA and CO_2 on NaX.

N_2 on CaA (195 K)		O_2 on CaA (195 K)		CO_2 on NaX (298 K)	
n [mol/kg]	q_{st} [kJ/mol]	n [mol/kg]	q_{st} [kJ/mol]	n [mol/kg]	q_{st} [kJ/mol]
0.222	29.8	0.059	18.7	0.205	48.7
0.307	29.3	0.091	18.9	0.361	48.2
0.394	28.9	0.126	18.8	0.523	47.8
0.581	27.7	0.162	18.4	0.730	46.2
0.679	27.6	0.196	19.1	0.979	45.4
0.785	27.1	0.231	18.7	1.300	44.2
0.892	26.5	0.262	18.3	1.600	43.2
1.000	26.2	0.295	17.6	1.890	41.6
1.110	25.7	0.328	17.0	2.200	40.2
1.220	25.2	0.366	17.6	2.510	38.8
1.330	24.8	0.411	16.7	2.750	38.1
1.450	24.6	0.460	17.5	3.000	37.8
1.600	24.7	0.515	16.6	3.260	38.2
1.760	24.2	0.576	16.3	3.460	37.2
1.930	22.8	0.643	16.5	3.700	36.6
2.100	22.2	0.732	16.8	3.980	36.5
2.250	21.9	0.832	16.5	4.140	35.2
2.400	21.8	0.940	16.4	4.270	32.8
2.550	20.9	1.080	16.3	4.410	35.3
2.690	20.6	1.230	16.4	4.500	33.3
2.910	20.2	1.560	16.1	4.570	33.8
3.180	19.8	1.760	15.7	4.670	32.4
3.410	19.5	1.970	15.7	4.780	33.0
		2.180	16.0	4.940	34.1
		2.380	15.6	5.080	32.5
				5.240	32.8
				5.380	32.2
				5.630	33.2
				5.820	31.0
				5.970	32.2

0.5 mol/kg. The limiting heat at zero coverage of CO_2 is 50 kJ/mol; heats decrease continuously with coverage to 33 kJ/mol at 5 mol/kg.

Adsorption Isotherms

A conventional volumetric apparatus was used to measure isotherms of O_2 and N_2 on CaA and CO_2 on NaX at three different temperatures. Approximately 0.5 g of zeolite sample was used for the determination of the isotherms. Zeolite powder was used for CaA and pellets with 20% binder were used for NaX. The samples were dehydrated using the same procedures as in the calorimeter. A leak rate of about 0.025 Pa/h was determined by evacuating the system and observing the increase of pressure with time. Compared to the average time allowed for sorption equilibrium (25 minutes) and the measured pressure range from 3 to 130 kPa, the influence of leakage on the results is negligible.

Isotherms measured at 35, 55, and 75°C for O_2 and N_2 on CaA, and for CO_2 on NaX, are presented in Tables 4–6 and Figs. 7–9, respectively. Loadings were measured on CaA up to 0.5 mol/kg for N_2 and 0.1 mol/kg for O_2; higher loadings could not be achieved without modifying the apparatus.

Heat Capacity

The heat capacity was determined by measuring the isosteric heat for N_2 and O_2 on CaA at two temperatures. Isosteric heats were calculated by Eq. (2) at the average temperature of 328 K using adsorption isotherm data in Tables 4 and 5. Since the isotherms were measured at low loading, the isosteric heats are effectively for the limit of zero loading: 24.5 kJ/mol for N_2 and 15.2 kJ/mol for O_2. These values at 328 K may be compared with the zero-coverage limits of the calorimetric measurements at 195 K on Fig. 11: 31 kJ/mol for N_2 and 19 kJ/mol for O_2, which coincide with the SIT data. Differences of heat capacities from Eq. (4) for the temperature range 195–328 K are $\Delta C_n = -5R$ for N_2 and $\Delta C_n = -3R$ for O_2. As mentioned previously, the variation of isosteric

Table 4. Isotherms of N_2 on CaA.

$T = 308$ K		$T = 328$ K		$T = 348$ K	
P [kPa]	n [mol/kg]	P [kPa]	n [mol/kg]	P [kPa]	n [mol/kg]
3.05	0.035	3.46	0.021	3.73	0.014
7.37	0.081	7.90	0.048	8.77	0.033
12.06	0.124	12.87	0.076	13.23	0.049
21.33[a]	0.201	21.52[a]	0.122	21.74[a]	0.079
24.15	0.222	24.84	0.138	26.41	0.093
33.82	0.289	34.39	0.182	35.18	0.123
48.56	0.379	49.95	0.249	49.51	0.166
62.88	0.453	66.13	0.310	65.55	0.211
75.27	0.514	77.75	0.350	77.63	0.241
92.61[a]	0.590	93.98[a]	0.403	93.29[a]	0.283
99.79	0.616	102.72	0.429	103.96	0.305
111.80	0.665	114.66	0.465	113.01	0.327
125.86	0.716	125.95	0.498	125.56	0.355

[a]Desorption.

Table 5. Isotherms of O_2 on CaA.

$T = 308$ K		$T = 328$ K		$T = 348$ K	
P [kPa]	n [mol/kg]	P [kPa]	n [mol/kg]	P [kPa]	n [mol/kg]
3.67	0.009	3.70	0.007	3.84	0.005
8.93	0.020	8.58	0.014	8.58	0.011
13.41	0.031	13.07	0.022	13.60	0.017
21.59[a]	0.052	21.58[a]	0.037	21.53[a]	0.027
25.67	0.061	25.68	0.043	26.11	0.033
32.97	0.076	33.04	0.056	33.54	0.042
41.83	0.095	42.94	0.071	43.94	0.054
55.14	0.122	56.01	0.090	57.24	0.070
69.75	0.150	70.19	0.113	70.78	0.085
81.17[a]	0.172	80.83[a]	0.129	79.44[a]	0.093
91.99	0.192	92.57	0.145	92.09	0.106
105.53	0.217	105.94	0.163	107.13	0.123
123.56	0.249	124.60	0.187	125.76	0.143

[a]Desorption.

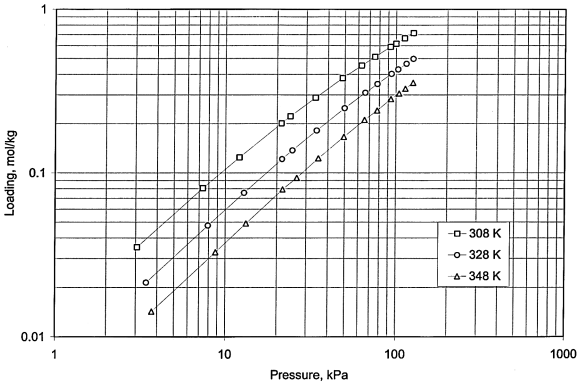

Figure 7. Adsorption isotherms of nitrogen on CaA at 308 K (squares), 328 K (circles), and 348 K (triangles) measured with volumetric apparatus.

Table 6. Isotherms of CO_2 on NaX.

$T = 312$ K		$T = 328$ K		$T = 348$ K	
P [kPa]	n [mol/kg]	P [kPa]	n [mol/kg]	P [kPa]	n [mol/kg]
0.01	0.059	0.02	0.037	0.02	0.018
0.02	0.104	0.03	0.059	0.03	0.024
0.03	0.154	0.04	0.084	0.04	0.033
0.06	0.247	0.06	0.118	0.07	0.052
0.08	0.379[a]	0.10	0.182	0.10	0.071
0.11	0.320	0.15	0.252	0.14	0.094
0.16	0.490	0.21	0.330	0.19	0.125
0.21	0.592	0.25	0.380	0.25	0.155
0.31	0.734	0.34	0.468[a]	0.35	0.211
0.40	0.844[a]	0.40	0.527	0.47	0.278
0.50	0.946	0.49	0.597[a]	0.55	0.314
0.59	1.014	0.51	0.619	0.74	0.391
0.76	1.138	0.51	0.612	1.02	0.479
1.01	1.283	0.61	0.678[a]	1.76	0.710
1.76	1.583	0.69	0.734	2.52	0.859
2.51	1.795	1.02	0.904	3.67	1.067
3.51	2.011	1.56	1.110	5.60	1.267
4.71	2.218	2.49	1.370	8.05	1.483
7.56	2.562	3.57	1.570	11.15	1.677
14.46	3.085	5.38	1.830[a]	14.97	1.906
10.72	2.843[a]	7.92	2.090	19.87	2.062
19.07	3.313	10.99	2.340	29.97	2.417
27.30	3.601	15.02	2.560[a]	40.11	2.557
38.74	3.873	20.03	2.790	50.04	2.679
45.91	4.000[a]	29.89	3.120[a]	61.63	2.871
56.81	4.147[a]	39.88	3.320[a]	64.87	3.009
76.17	4.349	49.92	3.490	73.34	3.053
96.37	4.498	60.38	3.570	80.10	3.116
119.15	4.636	75.10	3.760	91.77	3.234
138.11	4.725	88.24	3.800	109.43	3.396
		100.34	3.890	129.70	3.539
		118.80	4.010	140.80	3.607
		137.10	4.090		

[a]Desorption.

heat with temperature is largest at the limit of zero coverage.

7. Discussion

Figure 10 compares calorimetric measurements of isosteric heat with Eq. (2) using isotherms measured in the

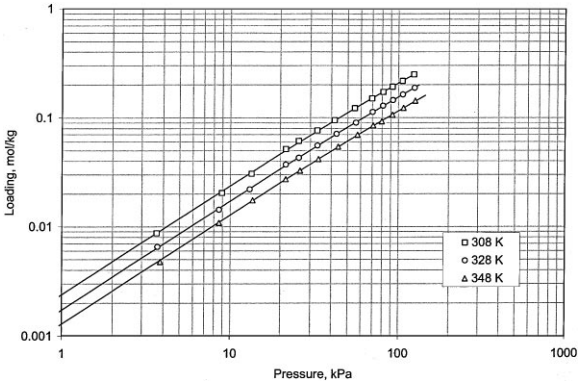

Figure 8. Adsorption isotherms of oxygen on CaA at 308 K (squares), 328 K (circles), and 348 K (triangles) measured with volumetric apparatus.

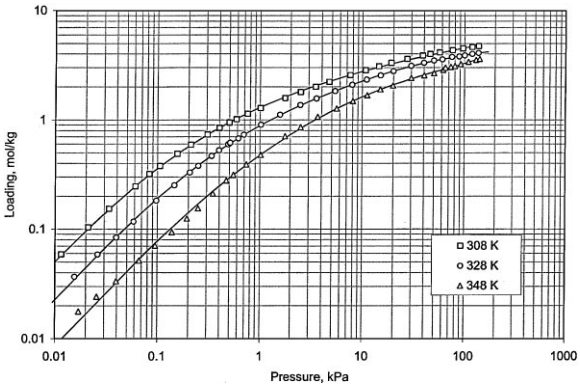

Figure 9. Adsorption isotherms of carbon dioxide on NaX at 312 K (squares), 328 K (circles), and 348 K (triangles).

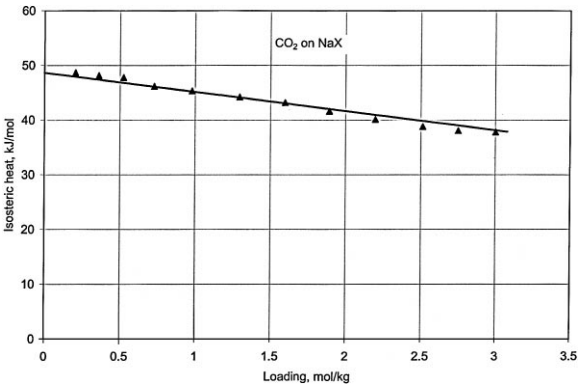

Figure 10. Isosteric heat for CO_2 on NaX. Experimental points: calorimeter at 298 K. Solid line: calculated from isotherms in Fig. 9 using Eq. (2).

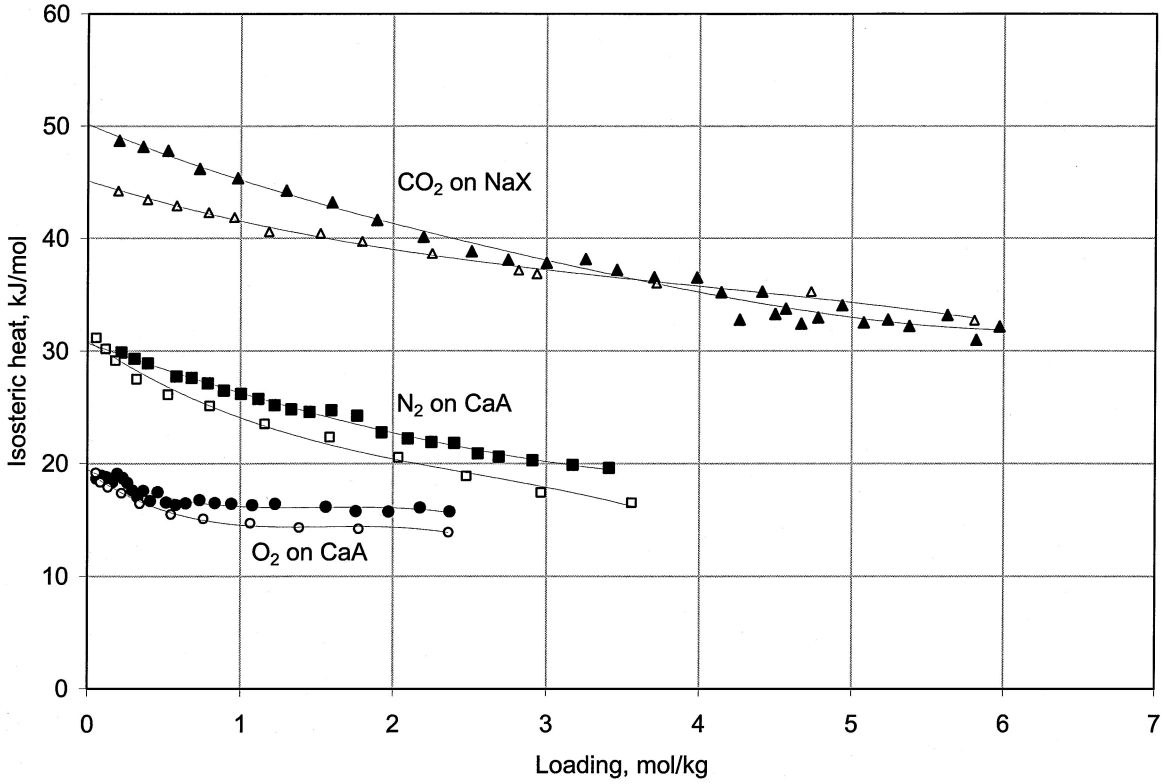

Figure 11. Comparison of heats of sorption measured by calorimetry (closed symbols) and SIT (open symbols). Temperature range for SIT heats are 60–250 and 70–200 K for N_2 and O_2 on CaA, respectively, and 155–310 K for CO_2 on NaX. Calorimetric heats were measured at 195 K for N_2 and O_2 on CaA and at 298 K for CO_2 on NaX.

temperature range 312–348 K. The average temperature of the adsorption isotherms is 328 K and the calorimetric measurements were at 298 K. The difference of 30 K between the two measurements is small and the effect of the temperature variable is negligible. The agreement of Eq. (2) with calorimetric measurements is excellent.

Figure 11 compares isosteric heats measured by the sorption isosteric technique (SIT) and by calorimetry. Isosteric SIT data are omitted for concentration regions which were not covered by calorimetric measurements. Overall the agreement is good but there is a systematic difference: in the range 1–3 mol/kg, the calorimetric heats are consistently higher than the SIT heats. The average difference is about 2 kJ/mol.

At high coverage in the range 3–6 mol/kg for the system CO_2/NaX, the calorimetric heats are somewhat lower than the SIT heats. At lower loading in the range 0–3 mol/kg, the SIT heats are less than the calorimetric heats; the largest difference of about 5 kJ/mol occurs at the limit of zero loading. The calorimetric heats were measured at 298 K and the SIT heats were measured in the range 155–310 K. Thus the difference between the SIT and calorimetric heats cannot be attributed to the variation of isosteric heat with temperature.

Figure 11 shows excellent agreement of SIT and calorimetric measurements of isosteric heat at the limit of zero loading for the systems N_2 and O_2 on CaA at 195 K. At higher loading, there is a systematic difference between SIT and calorimetric heats of about 2 kJ/mol. The SIT heats in the range of loading from 1–3 mol/kg were measured at an average temperature of 170 K; the calorimetric heats were measured at 195 K. Since the heat capacity is negative for these systems, the SIT heats should be higher, not lower, than the calorimetric heats. Thus the difference between the SIT and calorimetric heats cannot be attributed to the variation of isosteric heat with temperature.

In general, one expects lower heats from the SIT method if the isosteres deviate from linearity. However, the observed isosteres do not deviate from linearity, as shown on Figs. 3–5.

8. Conclusions

The isosteric method and calorimetry are in reasonable overall agreement. Depending on the types of sorption system and the concentration of sorption phases, both excellent agreement and differences between the heats from the two methods are observed. The reason for an average difference of about 2 kJ/mol remains to be identified.

Acknowledgment

Support to the University of Pennsylvania was provided by National Science Foundation Grant CTS-96-10030.

References

Bülow, M., *Stud. Surf. Sci. Catalysis*, **83**, 209–215 (1994).

Bülow, M. and P. Lorenz, in *Fundamentals of Adsorption*, A.I. Liapis (Ed.), pp. 119–128, Engineering Foundation, New York, 1987.

Coe, C.G., J.F. Kirner, R. Pierantozzi, and T.R. White, "Nitrogen Adsorption with a Divalent Cation Exchanged Lithium X-Zeolite," US Patent 5,258,058, granted Nov. 2, 1993.

Dunne, J.A., R. Mariwala, M. Rao, S. Sircar, R.J. Gorte, and A.L. Myers, *Langmuir*, **12**, 5888–5895 (1996a).

Dunne, J.A., M. Rao, S. Sircar, R.J. Gorte, and A.L. Myers, *Langmuir*, **12**, 5896–5904 (1996b).

Everett, D.H. and Powl, J.C., *J. Chem. Soc., Faraday Trans. 1*, **72**, 619–636 (1976).

Fitch, F.R., M. Bülow, and A.F. Ojo, "Adsorptive Separation of Nitrogen from Other Gases," US Patent 5,464,467, granted Nov. 7, 1995.

McKee, D.W., "Separation of an Oxygen-Nitrogen Mixture," US Patent 3,140,933, granted July 14, 1964.

Meier, W.M. and D.H. Olson, *Atlas of Zeolite Structure*, Third Revised Edition, Butterworth-Heinemann, Stoneham, MA, 1992.

Shen, D. and M. Bülow, *Microporous and Mesoporous Materials*, **22**, 237–249 (1998).

Shen, D., S.R. Jak, M. Bülow, and A.F. Ojo, *Stud. Surf. Sci. Catalysis*, **125**, 667–674 (1999).

Siperstein, F., R.J. Gorte, and A.L. Myers, *Langmuir*, **15**, 1570–1576 (1999).

Sircar, S., *J. Chem. Soc., Faraday Trans. I*, **81**, 1527–1540 (1985).

Sircar, S., *Ind. Eng. Chem. Res*., **31**, 1813–1819 (1992).

Valenzuela, D. and A.L. Myers, *Adsorption Equilibrium Data Handbook*, Prentice Hall, Englewood Cliffs, NJ, 1989.